

## – Supplementary material –

### Elastic anomalies across the $P2_1nm \rightarrow Pnnm$ structural phase transition in $\delta$ -(Al,Fe)OOH

Niccolò Satta<sup>1,2,3,\*</sup>, Giacomo Criniti<sup>1,†</sup>, Alexander Kurnosov<sup>1</sup>, Tiziana Boffa Ballaran<sup>1</sup>, Takayuki Ishii<sup>4</sup> and Hauke Marquardt<sup>2</sup>

<sup>1</sup>Bayerisches Geoinstitut, University of Bayreuth, 95447 Bayreuth, Germany

<sup>2</sup>Department of Earth Sciences, University of Oxford, OX1 3AN Oxford, United Kingdom

<sup>3</sup>Institute of Mineralogy, University of Münster, 48149 Münster, Germany

<sup>4</sup>Institute for Planetary Materials, Okayama University, Misasa, 682-0193 Tottori, Japan

<sup>†</sup>Current affiliation: Earth and Planets Laboratory, Carnegie Institution for Science, 20015 Washington, DC, USA

\*Corresponding author: Niccolò Satta ([nsatta@uni-muenster.de](mailto:nsatta@uni-muenster.de))

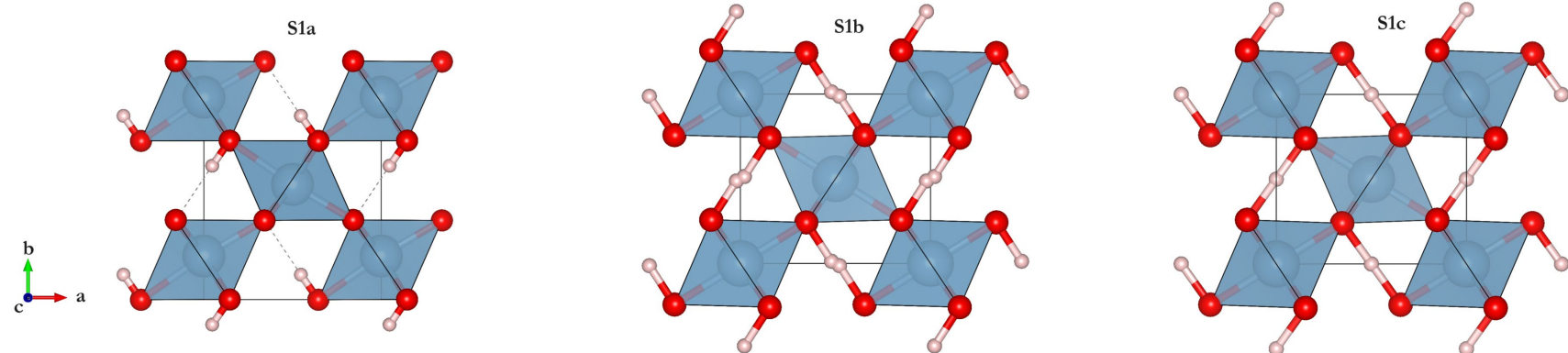
#### Contents

Figures

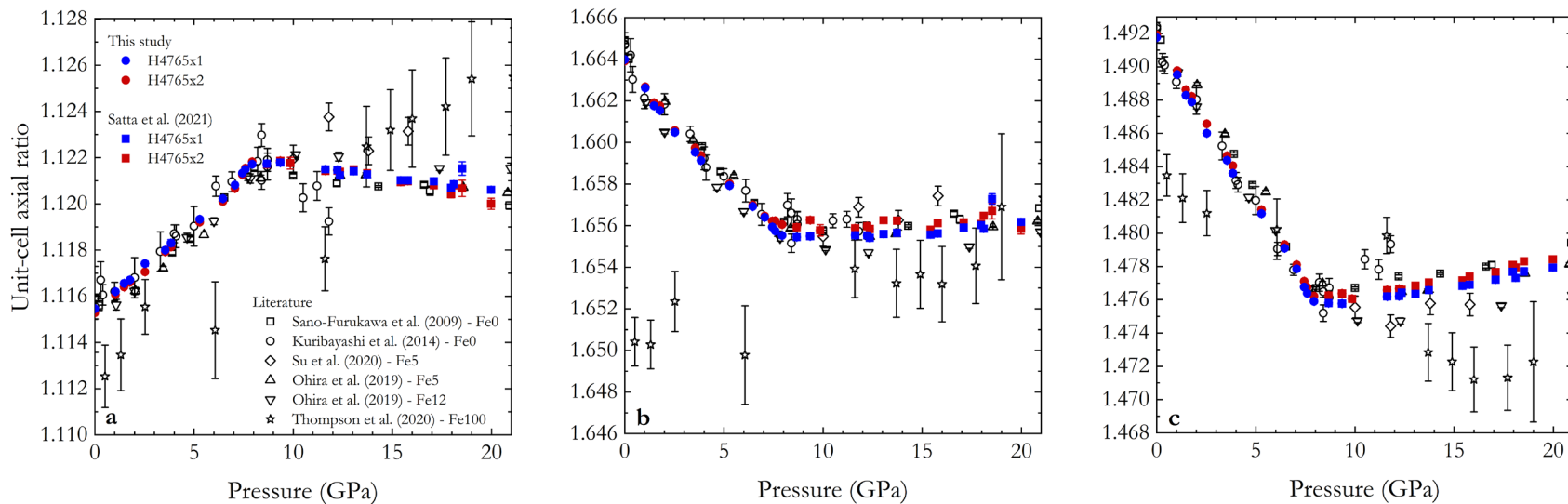
Tables

References

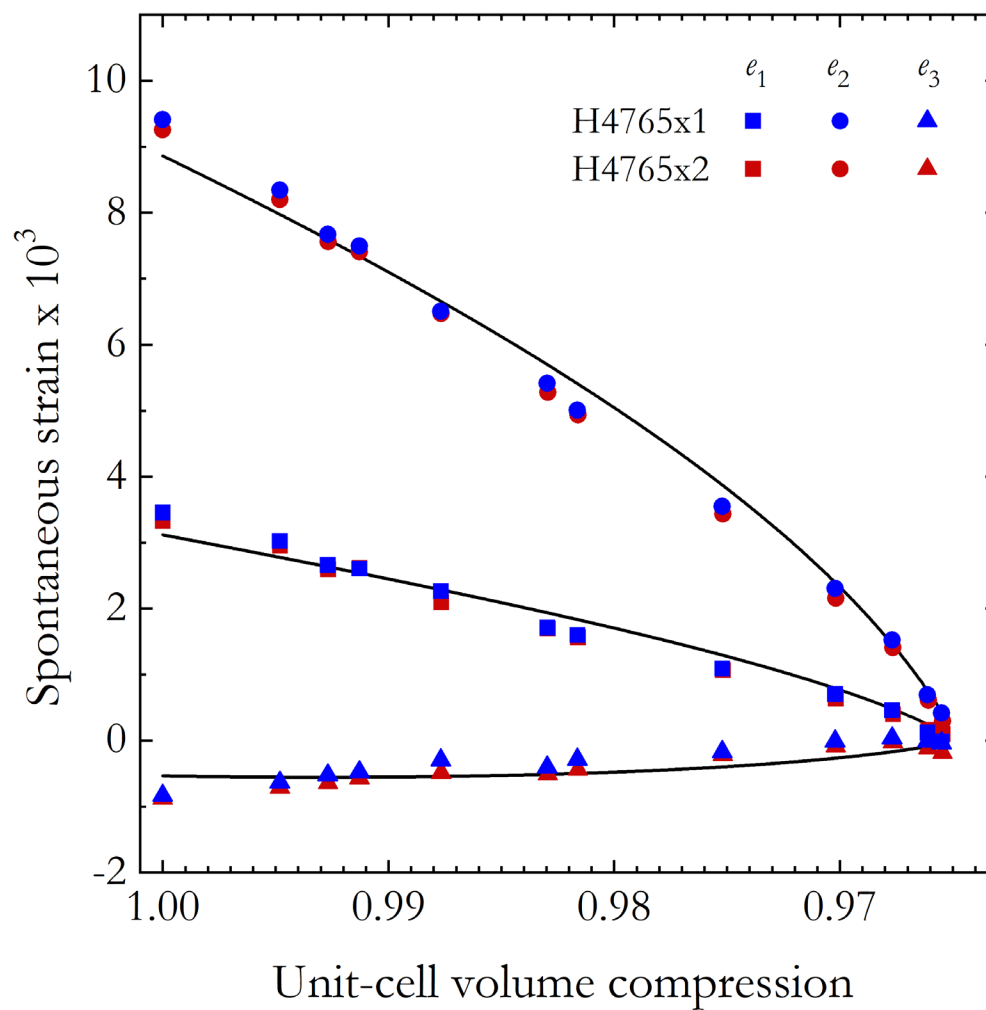
## Figures



**Supplementary Figure S1.** Structural models of  $\delta$ -AlOOH polymorphs: a) room pressure, structural data from Komatsu et al. (2006); b) at 9.5 GPa; c) at 18 GPa. Structural data of Figure S1b and c are from Sano-Furukawa et al. (2018).



**Supplementary Figure S2.** Unit-cell axial ratios as function of pressure ( $P$ ): a)  $a/b$ ; b)  $a/c$ ; c)  $b/c$ . Data from Satta et al. (2021) were obtained on the same samples of  $\delta$ -(Al<sub>0.97</sub>Fe<sub>0.03</sub>)OOH investigated in this study. Note that most uncertainties are smaller than the symbol size. Legend reported in a) applies to b) and c) as well.



**Supplementary Figure S3.** Spontaneous strains ( $e_1$ ,  $e_2$  and  $e_3$ ) in the  $P2_1nm$  phase of  $\delta$ -(Al<sub>0.97</sub>Fe<sub>0.03</sub>)OOH as function of unit cell volume compression ( $V/V_0$ ). Symbols show the experimentally observed spontaneous strain components, while solid curves results from the best fit to our data of a 2-4-6 Landau potential (Carpenter et al., 2003).

## Tables

**Supplementary Table S1.** Symmetry-constrained unit-cell parameters and volumes of  $\delta$ -(Al<sub>0.97</sub>Fe<sub>0.03</sub>)OOH determined in this study.  $P_{\text{ruby}}$  and  $P_{\text{calc}}$  are pressures (in GPa) determined from ruby luminescence (Dewaele et al., 2004) and from the BM3 parameters obtained in this study (Supplementary Table 2), respectively. SG, space group; PTM, pressure transmitting medium; Values at 10<sup>-4</sup> GPa are the same as in Satta et al. (2021).

	H4765x1 - Al <sub>0.972(7)</sub> Fe <sup>3+</sup> <sub>0.028(1)</sub> OOH					H4765x2 - Al <sub>0.977(9)</sub> Fe <sup>3+</sup> <sub>0.023(1)</sub> OOH						
$P_{\text{ruby}}$	$P_{\text{calc}}$	$a$ (Å)	$b$ (Å)	$c$ (Å)	$V$ (Å <sup>3</sup> )	$P_{\text{calc}}$	$a$ (Å)	$b$ (Å)	$c$ (Å)	$V$ (Å <sup>3</sup> )	SG	PTM
10 <sup>-4</sup>	10 <sup>-4</sup>	4.72227(5)	4.2335(1)	2.83793(5)	56.735(2)	10 <sup>-4</sup>	4.7197(2)	4.23182(4)	2.83650(5)	56.653(2)	$P2_1nm$	-
1.04(2)	1.02(1)	4.71151(9)	4.2210(2)	2.8338(1)	56.357(3)	1.01(1)	4.7092(1)	4.21943(4)	2.83228(5)	56.277(2)	$P2_1nm$	Ne
1.48(2)	1.50(1)	4.70627(8)	4.2150(2)	2.8321(1)	56.180(3)	1.50(1)	4.7040(2)	4.21353(6)	2.83048(7)	56.101(2)	$P2_1nm$	Ne
1.77(1)	1.76(1)	4.70372(5)	4.2121(1)	2.83095(5)	56.089(2)	1.74(1)	4.7018(3)	4.21076(6)	2.82939(8)	56.016(3)	$P2_1nm$	He
2.53(2)	2.53(1)	4.6961(1)	4.2027(4)	2.8282(2)	55.817(5)	2.54(1)	4.6933(3)	4.20151(9)	2.8263(1)	55.732(3)	$P2_1nm$	Ne
3.55(2)	3.60(2)	4.68561(6)	4.1911(2)	2.82346(6)	55.446(2)	3.59(2)	4.6835(4)	4.18949(8)	2.8219(1)	55.370(4)	$P2_1nm$	He
3.85(7)	3.89(2)	4.6829(1)	4.1875(6)	2.8225(2)	55.347(7)	3.88(2)	4.6807(2)	4.18616(8)	2.8208(1)	55.270(3)	$P2_1nm$	Ne
5.29(3)	5.31(2)	4.66990(5)	4.1721(1)	2.81672(5)	54.878(2)	5.29(2)	4.6678(3)	4.17058(6)	2.81528(8)	54.806(3)	$P2_1nm$	He
6.46(2)	6.44(3)	4.65988(6)	4.1598(2)	2.81237(7)	54.515(2)	6.44(3)	4.6576(3)	4.15815(6)	2.81086(8)	54.437(3)	$P2_1nm$	He
7.06(3)	7.06(4)	4.65464(4)	4.1529(1)	2.81010(5)	54.320(2)	7.05(4)	4.6524(2)	4.15143(4)	2.80862(6)	54.245(2)	$P2_1nm$	He
7.44(1)	7.57(4)	4.65046(6)	4.1473(2)	2.80836(7)	54.164(2)	7.54(4)	4.6487(4)	4.14592(5)	2.80678(9)	54.095(3)	$P2_1nm$	He
7.59(3)	7.76(5)	4.64883(6)	4.1452(2)	2.80769(7)	54.105(2)	7.73(4)	4.6474(4)	4.14372(5)	2.8060(1)	54.036(3)	$P2_1nm$	He
7.94(2)	8.09(5)	4.6461(1)	4.1420(3)	2.8064(2)	54.006(3)	8.06(5)	4.6447(3)	4.14035(4)	2.80470(7)	53.936(3)	$Pnnm$	He

**Supplementary Table S2.** Equation of State parameters of  $\delta$ -(Al<sub>0.97</sub>Fe<sub>0.03</sub>)OOH obtained in this study from fitting the unit-cell lattice parameters and volume as a function of pressure from both platelets with a BM3. EoS parameters reported in the literature are added for comparison. Note, however, that these previous experimental studies do not report linear EoS parameters, therefore no room  $P$  values for the unit-cell axes are reported in this table. -, not determined;

	H4765x1	H4765x2	Sano-Furukawa et al. (2009)	Ohira et al. (2019)		Thompson et al. (2020)
Composition	Al <sub>0.972(7)</sub> Fe <sup>3+</sup> <sub>0.028(1)</sub> OOH	Al <sub>0.977(9)</sub> Fe <sup>3+</sup> <sub>0.023(1)</sub> OOH	AlOOH	(Al <sub>0.832</sub> Fe <sub>0.117</sub> )OOH <sub>1.15</sub>	(Al <sub>0.908</sub> Fe <sub>0.045</sub> )OOH <sub>1.14</sub>	FeOOH
$a_0$ (Å)	4.7223(1)	4.7197(2)	-	-	-	-
$k_{a0}$ (GPa)	433(4)	433(4)	-	-	-	-
$k'_{a0}$	16.9(15)	16.9(15)	-	-	-	-
$b_0$ (Å)	4.2335(1)	4.2319(1)	-	-	-	-
$k_{b0}$ (GPa)	343(2)	343(2)	-	-	-	-
$k'_{b0}$	7.9(8)	7.9(8)	-	-	-	-
$c_0$ (Å)	2.8380(1)	2.8365(1)	-	-	-	-
$k_{c0}$ (GPa)	694(9)	694(9)	-	-	-	-
$k'_{c0}$	5(3)	5(3)	-	-	-	-
$V_0$ (Å <sup>3</sup> )	56.736(2)	56.654(2)	56.408(9)	57.85(2)	57.03(7)	66.14(4)
$K_{T0}$ (GPa)	150.6(11)	150.6(11)	152(2)	147(1)	152(7)	146(2)
$K'_{T0}$	3.5(4)	3.5(4)	4 (fixed)	4 (fixed)	4 (fixed)	4 (fixed)
EoS	BM3	BM3	BM2	BM2	BM2	BM2
$P$ range(GPa)	0-6.5	0-6.5	0-10	1.1-10.1	0-8.4	0-16

**Supplementary Table S3.** Elastic stiffness coefficients ( $c_{ij}$ ) of  $\delta$ -(Al<sub>0.97</sub>Fe<sub>0.03</sub>)OOH obtained in this study. Density ( $\rho$ ) are calculated averaging H4765x1 and H4765x2 density values. Pressure calculation from ruby fluorescence ( $P_{\text{ruby}}$ ) is based on the calibration of Dewaele et al. (2004). <sup>a</sup> and <sup>b</sup> label runs that used He or Ne as pressure medium, respectively. All values are in GPa, but the density that is in g/cm<sup>3</sup>.

$P_{\text{ruby}}$ (GPa)	$\rho$ (g/cm <sup>3</sup> )	$c_{11}$ (GPa)	$c_{22}$ (GPa)	$c_{33}$ (GPa)	$c_{44}$ (GPa)	$c_{55}$ (GPa)	$c_{66}$ (GPa)	$c_{12}$ (GPa)	$c_{13}$ (GPa)	$c_{23}$ (GPa)
<b><math>P2_1nm</math></b>										
10 <sup>-4</sup>	3.559(2)	360(2)	295(2)	414(2)	126.6(6)	126.8(4)	168.2(9)	41(2.4)	96(1.6)	61(2)
1.77(1) <sup>a</sup>	3.599(2)	391(1)	315(2)	418(2)	133.8(8)	131.8(8)	177.9(9)	55(1.6)	103(1.2)	61(2)
3.85(7) <sup>b</sup>	3.648(2)	417.7(15)	324(1.6)	443(2.5)	139.8(6)	134.8(3)	189.3(10)	56(1.7)	111.9(1.4)	63(2)
5.29(3) <sup>a</sup>	3.679(2)	425.8(6)	327(3)	439(2.5)	142.4(9)	135.7(3)	192.1(14)	60(2.5)	105(1.6)	69(2.4)
6.46(2) <sup>a</sup>	3.704(2)	440(1.6)	328(2.6)	446(2.3)	145.5(4)	137.4(9)	199.9(12)	57(2.4)	116.2(14)	73(2)
7.06(3) <sup>a</sup>	3.717(2)	450(2)	310(2)	457(2.7)	145.8(8)	138.2(4)	206(1.7)	47(2.2)	120(2)	58(2)
7.44(1) <sup>a</sup>	3.727(2)	450(3)	302(2.6)	464(3.7)	150.2(14)	140.0(8)	215(3)	36(4.7)	126(3)	50(4)
7.59(3) <sup>a</sup>	3.731(2)	449(2.5)	313(3)	482(5)	152.5(12)	141(1.8)	214(2.5)	45(4.7)	127(3)	61(3.7)
<b><math>Pnmm</math></b>										
7.94(2) <sup>a</sup>	3.738(2)	449.9(14)	477(4.4)	466(2.5)	151.1(6)	141.9(4)	211.2(12)	116(2.7)	113(2)	113(2)

**Supplementary Table S4.** Aggregate elastic properties obtained in this study for of  $\delta$ -(Al<sub>0.97</sub>Fe<sub>0.03</sub>)OOH. Density ( $\rho$ ) are calculated from EMPA results and unit-cell volumes constrained by X-ray diffraction on H4765x1 and H4765x2. The pressure obtained from the ruby fluorescence ( $P_{\text{ruby}}$ ) is based on the calibration of Dewaele et al. (2004). a and b superscripts label runs that used either He or Ne as pressure transmitting medium, respectively. R and V superscripts are used to label Reuss and Voigt bounds, respectively. H superscript is used to label Voigt-Reuss-Hill averaged values of the aggregate moduli; Aggregate velocities  $v_P$  and  $v_S$  are calculated using  $K_S^H$  and  $G^H$ .

$P_{\text{ruby}}$ (GPa)	$\rho$ (g/cm <sup>3</sup> )	$K_S^R$ (GPa)	$K_S^V$ (GPa)	$G^R$ (GPa)	$G^V$ (GPa)	$K_S^H$ (GPa)	$G^H$ (GPa)	$v_P$ (km/s)	$v_S$ (km/s)
<i>P2<sub>1</sub>nm</i>									
10 <sup>-4</sup>	3.559(2)	157(1)	162.7(9)	139.8(3)	142.4(4)	159.8(9)	141.1(3)	9.89(1)	6.30(1)
1.77(1) <sup>a</sup>	3.599(2)	169.0(8)	173.6(7)	146.5(3)	149.1(4)	171.3(7)	147.8(4)	10.12(1)	6.41(1)
3.85(7) <sup>b</sup>	3.648(2)	177.0(7)	183.0(7)	153.2(2)	156.4(4)	180.0(7)	154.8(3)	10.29(1)	6.51(1)
5.29(3) <sup>a</sup>	3.679(2)	179.1(12)	184.2(10)	154.8(3)	158.0(5)	181.6(11)	156.4(4)	10.30(2)	6.52(1)
6.46(2) <sup>a</sup>	3.704(2)	183(1)	189.5(9)	157.4(3)	161.1(5)	186.2(1)	159.3(4)	10.37(1)	6.56(1)
7.06(3) <sup>a</sup>	3.717(2)	175(1)	185.2(9)	159.2(3)	164.1(5)	180.1(9)	161.6(4)	10.32(1)	6.59(1)
7.44(1) <sup>a</sup>	3.727(2)	170(2)	183(1.6)	162.1(6)	168.1(9)	176(2)	165.1(7)	10.31(3)	6.66(1)
7.59(3) <sup>a</sup>	3.731(2)	178(2)	190(1.6)	163.6(7)	169.0(9)	184(2)	166.3(8)	10.43(3)	6.68(2)
<i>Pnnm</i>									
7.94(2) <sup>a</sup>	3.738(2)	230.7(12)	230.8(10)	167.6(3)	170.9(5)	230.7(11)	169.3(4)	11.05(2)	6.73(1)

## References

- Carpenter, M. A., Meyer, H.-W., Sondergeld, P., Marion, S., & Knight, K. S. (2003). Spontaneous strain variations through the low temperature phase transitions of deuterated lawsonite. *American Mineralogist*, 88(4), 534–546. <https://doi.org/10.2138/am-2003-0407>
- Dewaele, A., Loubeyre, P., & Mezouar, M. (2004). Equations of state of six metals above 94 GPa. *Physical Review B*, 70(9), 094112. <https://doi.org/10.1103/PhysRevB.70.094112>
- Komatsu, K., Kurabayashi, T., Sano, A., Ohtani, E., & Kudoh, Y. (2006). Redetermination of the high-pressure modification of AlOOH from single-crystal synchrotron data. *Acta Crystallographica Section E: Structure Reports Online*, 62(11), Article 11.  
<https://doi.org/10.1107/S160053680603916X>
- Sano-Furukawa, A., Hattori, T., Komatsu, K., Kagi, H., Nagai, T., Molaison, J. J., dos Santos, A. M., & Tulk, C. A. (2018). Direct observation of symmetrization of hydrogen bond in  $\delta$ -AlOOH under mantle conditions using neutron diffraction. *Scientific Reports*, 8(1), Article 1.  
<https://doi.org/10.1038/s41598-018-33598-2>
- Satta, N., Criniti, G., Kurnosov, A., Boffa Ballaran, T., Ishii, T., & Marquardt, H. (2021). High-Pressure Elasticity of  $\delta$ -(Al,Fe)OOH Single Crystals and Seismic Detectability of Hydrous MORB in the Shallow Lower Mantle. *Geophysical Research Letters*, 48(23), e2021GL094185.  
<https://doi.org/10.1029/2021GL094185>